ARTICLE NO. 79-7094R

A80-074

60001

Integral-Rocket Dual-Combustion Ramjets: A New Propulsion Concept

F. S. Billig,* P. J. Waltrup,† and R. D. Stockbridge‡
The Johns Hopkins University Applied Physics Laboratory, Laurel, Md.

A new propulsion concept for hypersonic volume-limited missiles is described—the integral-rocket dual-combustion ramjet (IRDCR). In essence, a "dump-type" subsonic combustion ramjet is embedded within the main supersonic combustion ramjet (scramjet) system to act as a fuel-rich hot-gas generator for the latter and thus permit use of a hydrocarbon fuel rather than highly reactive borane based fuel. By packaging rocket-boost-phase propellant in the scramjet combustor, the volumetric efficiency of the propulsion system is improved. The new techniques required to design the IRDCR engine cycle and evaluate its performance are developed and discussed in the framework of exemplary calculations for a particular family of inlet designs and for flight at Mach numbers 4-7 at a constant flight dynamic pressure of 5000 lb_f/ft^2. The sensitivity of engine performance to inlet operating characteristics is discussed in terms of maximum thrust and engine efficiency. In general, IRDCR performance characteristics are intermediate to those of conventional ramjets and scramjets with some of the advantages of each.

Nomenclature

A	= area
$C_{D,\text{add}}$	= additive drag coefficient, Eq. (12)
C_F	= net thrust coefficient, Eq. (10)
C_T	= thrust coefficient, Eq. (11)
ER	= equivalence ratio
g	= acceleration due to gravity
h	= enthalpy
I_{spn}	= net specific impulse, Eq. (13)
M	= Mach number
p	= pressure
q	= dynamic pressure
R	= gas constant
Q_w	= heat transfer rate
s	= entropy
S_d	= length of shock-expansion zone, Fig. 10
S_0	= separation distance, Fig. 10
T	= temperature
u	= velocity
$\dot{w}_f$	= fuel flow rate
Z	= sonic flow parameter, Eq. (1)
$\hat{Z}$	= normalized sonic flow parameter, Eqs. (2) and (3)
Z_0	= altitude
γ	= ratio of specific heats
ϵ	= exponent in pressure area relationship
$\bar{\epsilon}$	= value of ϵ satisfying Eq. (9)
ρ	= density
τ	= shear stress

Superscripts

$( )^*$	= conditions at sonic point
$\overline{( )}$	= average conditions
$( )'$	= conditions downstream of a normal shock

Subscripts

b,base	= base area, Fig. 10
ce	= combustor exit
ci	= combustor inlet
ex	= engine exit
f	= fuel
gg	= gas generator
i	= engine inlet
max	= maximum or critical
s	= after shock
sj	= scramjet
t	= stagnation
tot	= total engine
w	= wall
0	= freestream
2	= plane of cowl lip
3	= start of 2D-3D zone, Fig. 10
4	= end of 2D-3D zone, Fig. 10

Introduction

THE integral-rocket dual-combustion ramjet (IRDCR) is a new propulsion concept that is well suited for hypersonic volume-limited missile systems. It combines the high booster-propellant-packaging efficiency inherent to integral-rocket ramjets with the high performance at high speed characteristics available from supersonic combustion ramjets. In this new design a "dump-type" subsonic combustion ramjet is imbedded within a main supersonic combustion ramjet system to act either as a hot-gas pilot or a fuel-rich gas generator and thus to permit the use of conventional hydrocarbon fuels not hitherto usable over the entire range of desired operating conditions of a hypersonic ramjet missile.

Figure 1 is a schematic illustration of one possible configuration of an IRDCR. Part a shows the engine configuration during the initial rocket boost phase. The inlet is covered by a low-drag fairing. The ramjet combustion chambers are filled with a solid rocket propellant. Frangible closures cover the annular air passages to the main combustor and the dump combustor. (For some missions a tandem booster will be required to obtain the desired speed for transition to ramjet operation.) At burnout of the integrated boost propellant, the rocket nozzles, frangible port covers, and nose fairings are ejected, and the engine now operates as a fuel-combustion ramjet.

Presented as Paper 79-7094 at the Fourth International Symposium on Air Breathing Engines, Lake Buena Vista, Orlando, Fla., April 1-6, 1979; submitted Aug. 13, 1979; revision received March 14, 1980.

Index category: Airbreathing Propulsion.

*Assistant Division Supervisor, Aeronautics Division. Fellow AIAA.

†Supervisor, Supersonic Combustion Section. Associate Fellow AIAA.

‡Engineer, Supersonic Combustion Section. Member AIAA.

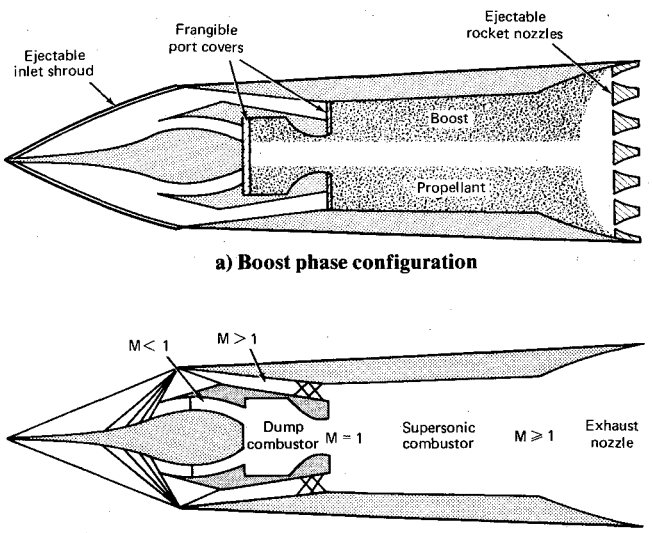

Fig. 1 Schematic illustration of integral-rocket dual-combustion ramjet.

Part b of Fig. 1 shows schematically the engine operating as a dual-combustion ramjet, with particular emphasis on the shock structure in the external/internal compression system. Air is initially compressed by an axisymmetric external compression surface. The inner cowl lip subdivides this compressed air, ducting a smaller fraction to a dump-type subsonic combustor. The cross-sectional area of the duct increases in the streamwise direction to provide stable throttling by positioning of the normal shock structure. For clarity, this shock structure is represented by a single wave perpendicular to the flow direction. This portion of the inlet is operated supercritically because subcritical operation would produce undesirable interactions with the major portion of the external compression field.

The major portion of the flow bypasses the inner duct and is turned towards the engine axis supersonically by the outer cowl compression surface. In this simplified illustration, the compression is represented by a single oblique wave emanating from the cowl lip. Variants in the inlet design include cases where the external compression of either the inner or the outer flow is increased relative to other flow. For the former, the innerbody compression surface could be curved outward downstream of the last external compression wave shown in Fig. 1b and for the latter, the external surface of the inner cowl lip could be curved outward, downstream of the same external compression wave.

The final shocks in the external duct which are depicted as two sets of intersecting oblique waves are due to the combustor/inlet interaction which will be present for most operating conditions of the engine (see Refs. 1-4). The design of the outer annular duct includes an isolator section to prevent the combustion-induced disturbances from interacting with the external compression field of the inlet.

Superficially, it would appear that this engine concept is just an arbitrary combination of two ramjet cycles, a subsonic dump-type and a scramjet, and would be expected to yield performance that would lie within the range that would be associated with single cycle ramjets of the two types and have no particular advantage over one or the other. In fact, if the range of operating Mach number, M_0, does not exceed 5-6, the subsonic combustion integral-rocket ramjet would be the preferred cycle. Moreover, if the ramjet only had to function at $M_0 > 6$-7, then the scramjet would be preferred. On the other hand, if the airbreather must use a conventional hydrocarbon fuel and function over a wide Mach number range, say from below $M_0 = 4$ to above $M_0 = 6$, then the IRDCR is preferred. This arises from the fact that a fixed-geometry subsonic-combustion ramjet designed to produce acceptable performance at $M_0 = 4$ operates very inefficiently during cruise at $M_0 > 6$, and a scramjet, designed to operate solely on liquid hydrocarbon fuels without auxiliary piloting, has not been demonstrated at conditions simulating flight at $M_0 \leq 4$ in the tropopause. Therein lies the efficacy of IRDCR; the dump combustor can act either as a pilot or a gas generator to assure that heat can be efficiently released in the supersonic combustor, even when M_0 is low. If it is operated as a pilot, fuel is added to both streams; if it is operated as a gas generator, all or nearly all of the fuel is added within it, and the main combustor becomes a supersonic "afterburner." The latter approach requires the dump combustor to operate very fuel-rich. Heretofore, efficient operation of a scramjet engine at M_0 4-5 has been restricted to hydrogen,[5] alkylated boranes[6] or with a supplemental oxidizer (chlorine trifluoride by the Marquardt Co.[7]), or with a separately-fueled near stoichiometric pilot (by the United Aircraft Research Laboratories[8]). In subsonic flow, Mestre and Ducourneau[9] demonstrated the feasiblity of fuel-rich combustion of kerosine and air at equivalence ratios as large as 7.7 at conditions corresponding to $M_0 = 3$-4.

To develop the arguments that led to the aforementioned conclusions regarding the merits of the IRDCR relative to conventional subsonic combustion ramjets or scramjets, it is necessary to select a particular range of operating conditions and in turn certain geometric constraints. Moreover, certain simplifying assumptions regarding the chemical composition of the combustion products and the effects of wall friction in the inlet and combustor will be made. Thus, the absolute values of performance that will be presented are subject to further refinements which can readily be made but are beyond the scope of this study. This analysis will be limited to fixed geometry of the engine components and operation with the vehicle at zero angle of attack. It will be assumed that the engine must operate over the Mach number range of 4 to 7 and over a range of overall fuel/air equivalence ratio (ER) of 0.25 to 1.0, where the lower value could represent cruise at constant speed and the upper limit an accelerative and/or climb-out mode of operation.

Flight conditions based on a constant dynamic pressure, $q_0 = 5000$ lb/ft^2, and an ICAO standard atmosphere[10] were assumed.

The fixed-geometry constraint leads not only to considerable compromise in performance at off-design operating conditions but requires special consideration in obtaining a suitable match of the inlet and combustor geometries.

Inlet Design

Figure 2 depicts the external compression field of the inlet family considered in this study. The cone inlet is simply a 12.5 deg half-angle conical compression surface. Inlets A through E have the same initial 12.5 deg half-angle conical compression followed by an isentropic turning to maximum surface angles of 15.5, 18.0, 21.0, 27.1, and 34.15 deg, respectively. The design point for the inlets was chosen to be $M_0 = 7$. Figure 2a shows the compression surface corresponding to the maximum turning at $M_0 = 7$. The last left running characteristic from each of the other cases is also shown so these inlets can easily be depicted by simply extending the surface beyond this characteristic to the plane of the cowl lip as a simple cone. All of the flowfield calculations were based on the inviscid flow of air with a variable specific heat. The compression field of each of these inlets was then computed at lower M_0 as typified by the sketch shown in Fig. 2b. For each inlet at the selected M_0 values, the total inlet air capture ratio A_0/A_i, additive drag $C_{D,\text{add}}$, and the Mach number distribution in the cowl lip plane were determined. At $M_0 = 7$ a point was located on the final characteristic which subdivided the flow in the proportion 1:3, i.e., 25% of the

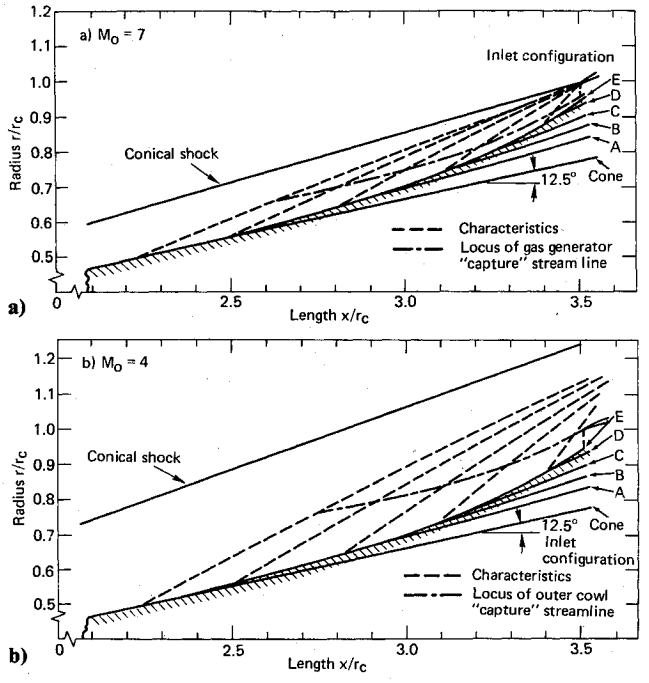

Fig. 2 Family of inlet compression fields.

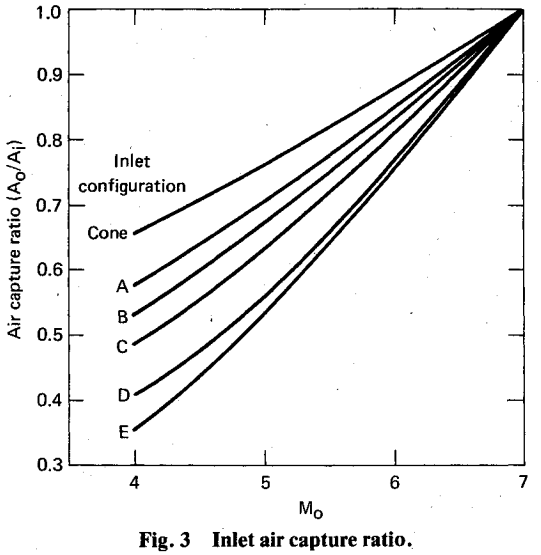

Fig. 3 Inlet air capture ratio.

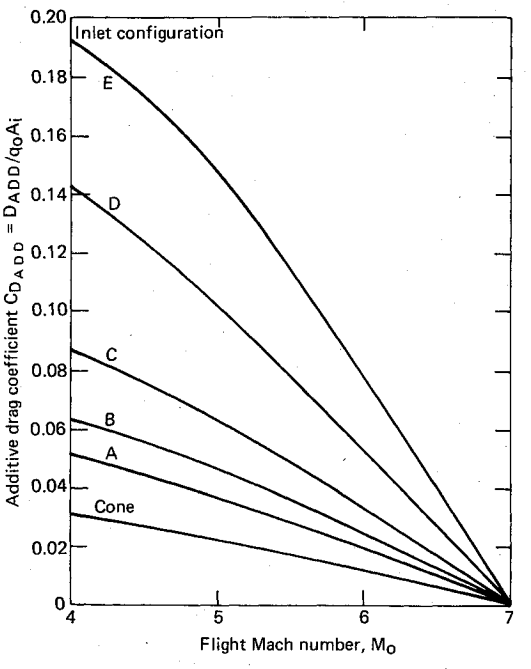

Fig. 4 Additive drag coefficients for family of inlets.

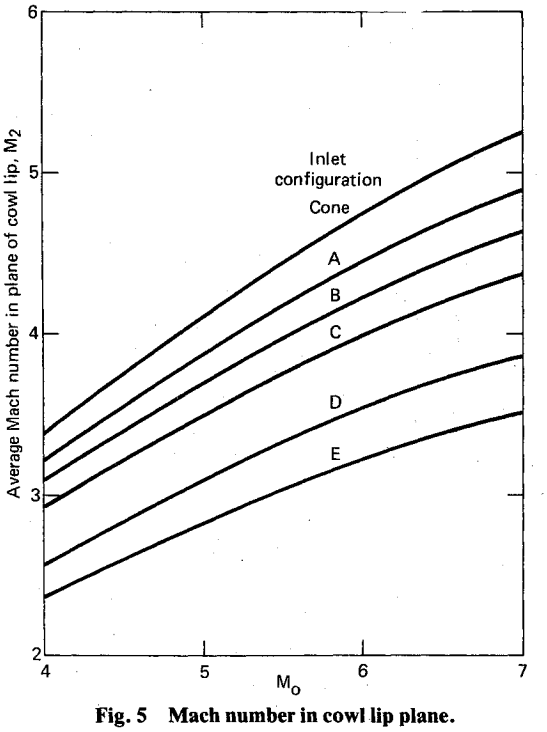

Fig. 5 Mach number in cowl lip plane.

flow is contained in this inner streamtube. With the flow thus subdivided, the mass split at lower Mach numbers was determined and the average Mach number $\bar{M}_2$ and local flow direction in the respective cowl lip planes were found. As it turned out, the variation in the proportion of gas generator flow to total inlet flow at $M_0 < 7$ was no greater than 0.2%, so it was assumed to be 25% at all M_0.

Figure 3 shows the variation of A_0/A_i as a function of M_0 for each of the inlets. Figure 4 shows $C_{D,\text{add}}$. Figure 5 shows the computed values of $\bar{M}_2$ for each of the inlets over the range of $4 \leq M_0 \leq 7$.

Figure 6 is a plot of the critical, i.e., normal shock on lip, pressure recovery of the gas generator $\bar{p}_{t_2}{}'/p_{t_0}$ vs M_0 for each inlet configuration.

In the outer duct which supplies air to the main combustor the flow remains supersonic to the combustor inlet station, at which the Mach number is M_{ci}. For this study, it was assumed that the flow was further contracted internally by 1/6, but with a corresponding loss of 10% in total pressure recovery, i.e., $A_{ci}/\bar{A}_{2_{si}} = 0.833$ and $p_{t_{ci}}/\bar{p}_{t_2} = 0.9$. Henceforth in the discussion the superscript bars denoting average flow properties at a station in the flowfield are dispensed with, but the meaning is implied. With these assumptions, conditions at the scramjet combustor inlet can be obtained. Figure 7 shows values of M_{ci} for the six inlet configurations studied.

Gas Generator Design

Consistent with the constraint of a fixed engine geometry, a nozzle with a specified throat area must be selected for each inlet geometry. For this calculation it is convenient to use the sonic gas flow parameters given in Ref. 11 for the products of combustion of Shelldyne-H and air which were obtained assuming isentropic expansion of the products in local thermodynamic equilibrium. The assumption of local

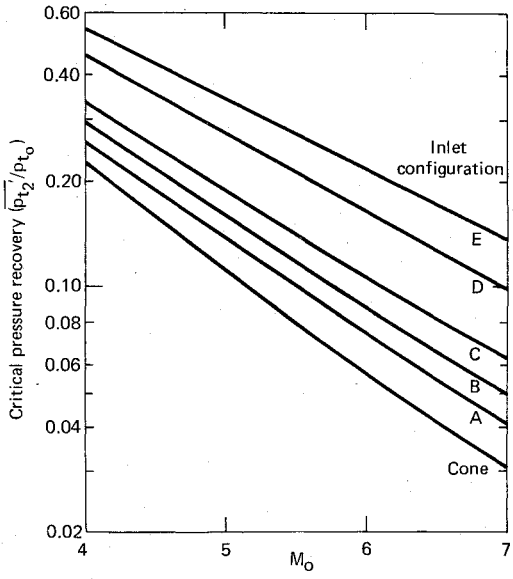

Fig. 6 Critical pressure recovery of gas generator inlet.

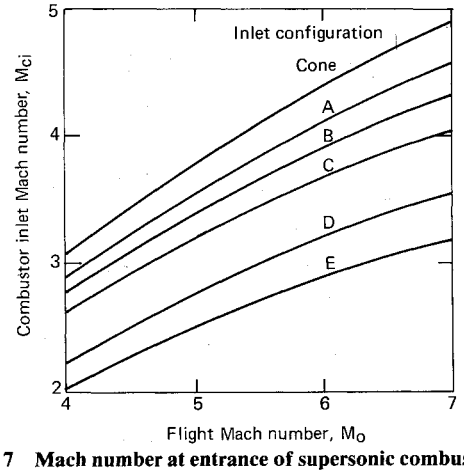

Fig. 7 Mach number at entrance of supersonic combustor.

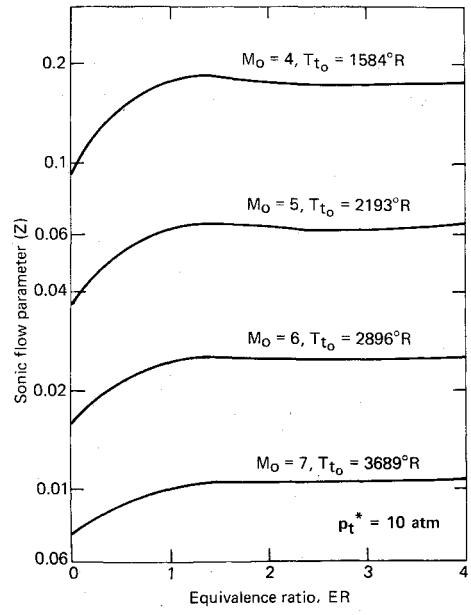

Fig. 8 Sonic flow parameter, Z.

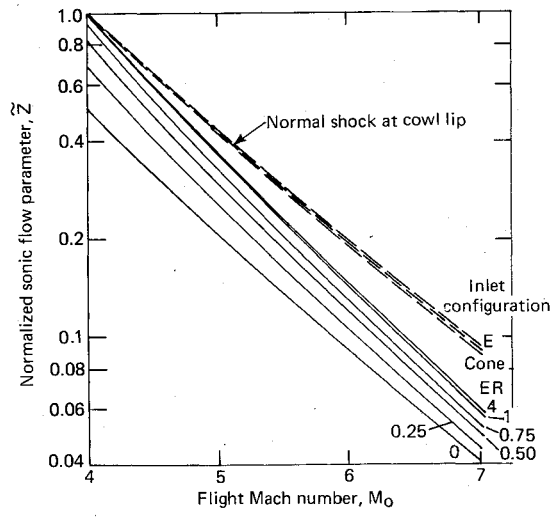

Fig. 9 Normalized sonic flow parameter.

thermodynamic equilibrium was also used to determine the flow properties in the discharge plane of the supersonic combustor and in the exhaust nozzle. Shelldyne-H (RJ-5) was selected as the fuel as it is representative of a "conventional" high density hydrocarbon fuel. In all calculations presented herein, no degradation in performance due to combustion inefficiency has been assumed, so the absolute values for performance are accordingly optimistic.

Values of a sonic flow parameter defined as

$$Z \equiv A^* p_t^* / A_0 p_{t_0} \tag{1}$$

were computed for the range of equivalence ratios $0 \leq ER \leq 4$ for free-stream total temperatures of 1584°R, 2193°R, 2896°R, and 3689°R, which correspond, respectively, to flight speeds $M_0 = 4$, 5, 6, and 7. Values of Z are shown in Fig. 8 for $p_t^* = 10$ atm. The total pressure in the combustor varies from about 6-20 atm for the cases studied herein, but Z is nearly invarient with p_t^* over this range so the weak pressure dependence was neglected. The nearly constant value of Z for $ER > 1$ at a constant T_{t_0} has considerable significance in the operating characteristics of the inlet for the gas generator. Equation 1 shows that if Z is constant, then p_t^*/p_{t_0} is constant for a given A^* and M_0. Thus, if A^* is selected such that the inlet is operating near critical at $ER = 1$, it will operate near critical over the entire operating range $1 \leq ER \leq 4$, therefore there is no decrement in inlet performance due to throttling.

On the other hand, for a fixed A^* and near critical operation of the inlet at $ER = 1$ in a conventional subsonic combustion ramjet, Z drops off considerably in the corresponding operating range $0.25 \leq ER \leq 1$. Thus, from Eq. 1, p_t^*/p_{t_0} must also proportionally decrease with Z, so the inlet must operate substantially supercritically as the engine is throttled back. The variation of Z with M_0 leads to a matching requirement for the inlet and combustor, that involves both the air capture and pressure recovery characteristics of the inlet. Ideally, A^* would be selected such that the inlet would operate near critical at all flight conditions and ER's. Actually, this is difficult to achieve and instead, A^* must be selected such that the inlet is never required to exceed critical pressure recovery. Thus, A^* must be "oversized" for some operating conditions, as is the case with a conventional subsonic combustion ramjet, both at lower ER and higher M_0. Figure 9 depicts this point and shows the degree of "matching" that occurs with the inlets studied herein. Here, the sonic flow parameter is normalized by the maximum value of Z which corresponds to $M_0 = 4$, $ER = 1$; that is,

$$\tilde{Z} \equiv Z/(Z)_{M_0=4,\ ER=1} \tag{2}$$

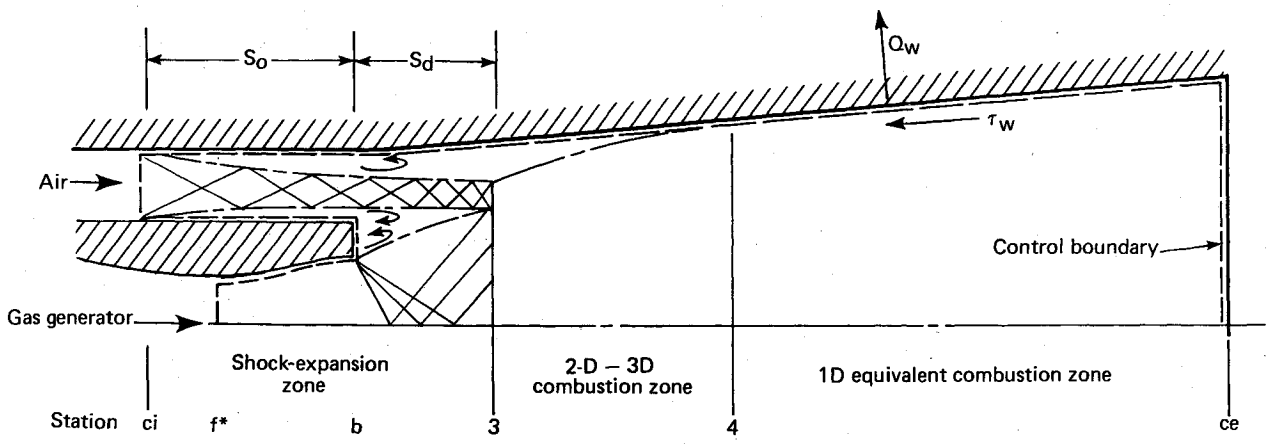

Fig. 10 Theoretical model for combustion analysis.

which can be matched with $\bar{Z}$ for a given inlet, viz.

$$\bar{Z}=\frac{(p_t^*/p_{t_2}')}{(p_t^*/p_{t_2}')_{M=4,ER=1.0}}\frac{(p_{t_2}'/p_{t_0})_{\max}}{(p_{t_2}'/p_{t_0})_{\max@M_0=4}}\times\frac{(A_0/A_i)_{M_0=4}}{(A_0/A_i)} \tag{3}$$

where the subscript max refers to the critical pressure recovery. The lead term in Eq. (3) accounts for total pressure losses downstream of the normal shock. In this study an additional loss of 10%, invariant with M_0 and ER was assumed, thus $p_t^*/p_{t_2}'=0.90$ and the lead term is unity. The curves for $ER=1$-4 are nearly superposed and those for $ER<1$ are lower, corresponding to the results shown in Fig. 8. The curves for the inlet configurations are also nearly superposed. Matching of the inlet and combustor only occurs at $M_0=4$ over the range $1\leq ER\leq 4$. For all other conditions all inlets must operate supercritically. Had the inlet design characteristics been such that the curve fell below the combustor curve, then A^* would have to be raised correspondingly so as not to exceed critical total pressure recovery. Since all inlet configurations studied had nearly the same $\bar{Z}$, no argument can be made at this point regarding the selection of a particular inlet. Indeed, the pressure recovery that could have been available to the gas generator cannot be used at $M_0<4$ because A^* must be selected to accommodate $ER=1$ at $M_0=4$. Thus, in the subsequent calculations for the conditions at the gas generator discharge in the IRDCR and for the comparative case of the subsonic combustion ramjet, inlet pressure recoveries must be degraded by the ratio of $\bar{Z}$ at conditions other than $M_0=4$, $ER=1$-4.

Supersonic Combustor Analysis

The method for analyzing the flow in the supersonic combustor is an extension of the method first presented in Ref. 1. A schematic representation of the flow model is depicted in Fig. 10. The indicated control boundary, selected such that the flow in the entrance and exit planes can be considered one-dimensional, has entrance conditions which correspond to M_{ci} for the main combustor air flow and to $M^*=1.0$ for the gas generator exhaust flow and has exit conditions which correspond to M_{ce}. Within the control boundary, however, the flow is permitted to be highly nonuniform at any cross-sectional plane. Three major regions of the flow are defined. A shock-expansion zone is followed by a highly nonuniform two- or three-dimensional combustion zone which eventually blends into a combustion zone that is nearly one-dimensional at a given flow station. In the shock-expansion zone, the flow from the gas generator and the supersonic air inlet adjust to a matched pressure condition, p_s, that is consistent with the shock-combustion model postulated in Ref. 1. In general, this adjustment is manifested as an expansion of the gas generator exhaust and a compression of the air inlet flow. Situations also exist which require a compression wave in the supersonic portion of the gas generator nozzle, thus the sonic point in the gas generator has been selected as the entrance station in the control boundary. When a shock is located upstream of the exit plane of the gas generator nozzle and/or if there is a base region between the two incoming streams, there is a separated zone and p_s is assumed constant on this portion of the control boundary. The compression field in the air stream also causes local separation that extends a distance S_0 upstream of the discharge plane of the gas generator. This distance, S_0, as well as the downstream extent of the shock-expansion region, S_d, have been determined for conventional supersonic combustors,[4] but have not yet been obtained for the IRDCR configuration. Downstream of the shock-expansion zone mixing and combustion commence in a region of large radial and circumferential gradients and, in general, the effective cross-sectional area of the flow is smaller than the local cross-sectional area of the duct. Finally, combustion is completed in a zone which can be approximated as one-dimensional with a cross-sectional area equal to the local physical area of the duct.

The governing equations are:

Conservation of Mass:

$$\rho_{ci}u_{ci}A_{ci}+\rho_f^*u_f^*A_f^*=\rho_{ce}u_{ce}A_{ce} \tag{4}$$

Conservation of Momentum:

$$P_{ci}A_{ci}+P_f^*A_f^*+\int p_w\mathrm{d}A-\tau_wA_w=\rho_{ce}u_{ce}^2A_{ce}-\rho_{ci}u_{ci}^2A_{ci}-\rho_f^*u_f^{*2}A_f^* \tag{5}$$

Conservation of Energy:

$$\rho_{ci}u_{ci}A_{ci}(h_{ci}+u_{ci}^2/2)+\rho_f^*u_f^*A_f^*(h_f^*+u_f^{*2}/2)=\rho_{ce}u_{ce}A_{ce}(h_{ce}+u_{ce}^2/2)+Q_w \tag{6}$$

Equation of State:

$$h,s,\rho=f(p,T) \tag{7}$$

As in the case of the gas generator, local thermodynamic equilibrium is assumed at *ce* with product compositions and property relationships for Eq. (7) obtained from an equilibrium gas computer program based on Ref. 12.

To solve this set of equations for a given set of initial conditions and combustor areas, the wall pressure force $\int p\mathrm{d}A$,

shear force $\tau_w A_w$, and heat loss to the wall Q_w must be defined. References 5 and 13 give methods for computing these quantities in reacting supersonic flow for typical scramjet combustors, but the veracity of these techniques for the IRDCR configuration has not yet been demonstrated. In flight-type hardware with passive thermal protection, Q_w will be small compared to the heat release and therefore is neglected in this study. For simplicity $\tau_w A_w$ is also neglected here, which is consistent with the approach taken in the analysis of the inlet.

For the general solution the wall pressure forces are determined as follows:

1) In the divergent portion of the gas generator nozzle, the isentropic pressure distribution is used, either throughout for most cases, or up to the point where the flow has been separated by a compression wave for $p_s/p_f \gtrsim 3$. In the latter case the conditions for separation are found using the method of Ref. 14 for shock-separated turbulent boundary layers.

2) In the separated portion of the gas generator nozzle, if it exists, and on the base area A_{base}, $p = p_s$. For simplicity in this study, the gas generator discharge was taken as sonic and no base region was considered.

3) In the region *b*-4, on the outer wall the correlating formula of Ref. 4 could be used, but as previously stated, these data correlations may not be valid for IRDCR. Thus, for this study the exponential distribution used in region 4-*ce* is extended to include region *b*-4.

4) In region 4-*ce* the simple exponential relationship $pA^{\epsilon/\epsilon-1} = \text{constant}$, where ϵ is an arbitrary constant, first suggested by Crocco,[15] is used. Numerous tests in supersonic combustors (see e.g., Ref. 5) have established the credence of this method.

With this assumption and the condition $dT_t/T_t = 0$ at the combustor exit, the general constraint that

$$\frac{dA}{A} = \frac{(M^2-1)}{2+(\gamma-1)M^2}\frac{dM^2}{M^2} \tag{8}$$

yields an explicit relationship between $\bar{\epsilon}$ and M_{ce}, viz.

$$\bar{\epsilon} = \frac{\gamma_{ce} M_{ce}^2}{1+(\gamma_{ce}-1)M_{ce}^2} \tag{9}$$

where $\bar{\epsilon}$ refers to the value of ϵ that satisfies Eq. (9). Typical values of $\bar{\epsilon}$ range from 1.5 to ∞ (see Ref. 1).

With this constraint, unique solutions of Eqs. (4-7) exist for most given initial conditions and engine geometries. The procedure involves the selection of an initial value for p_s, or ϵ, solving for M_{ce}, γ_{ce} and testing of Eq. (9). Generally, several iterations are required for closure and difficulties can arise in convergence. Nonetheless, routines have been developed that result in a cost of about a dollar for one case on a large digital computer.

The initial conditions for which Eq. (9) can not be satisfied occur for low M_{ci} and high *ER*. That is, for a selected combustor area ratio A_{ce}/A_{ci} and a particular low value of M_{ci}, solutions satisfying Eq. (9) will exist at low values of *ER*. As *ER* increases, the corresponding value of p_s/p_{ci} increases, until p_s/p_{ci} corresponds to the pressure rise of a normal shock and, in fact, the flow in the combustor is initially subsonic and accelerates to $M_{ce} > 1$ at the combustor exit.[1] For higher heat release rates, solutions exist but the constraint imposed by Eq. (9) need not be, nor is it, met. The limiting case corresponds to a solution with $M_{ce} = 1$. Conversely, if an engine operating requirement is specified, i.e., the minimum M_{ci} which corresponds to the minimum M_0 and the maximum *ER*, then this condition requires the maximum A_{ce}/A_{ci} at $M_{ce} = 1$ and, therefore, this specifies the combustor exit size for a fixed geometry IRDCR. For the cases studied herein, the condition $M_0 = 4$, $ER = 1$ is the limiting case where the values of M_{ci} at $M_0 = 4$ are shown in Fig. 7.

A similar set of constraints and design conditions must be met in a scramjet. Thus, in a scramjet, as in an IRDCR, A_{ce} is set by $M_{ce} = 1$ with a normal shock at M_{ci}. In a conventional ramjet, as in the gas generator of IRDCR, the area at the sonic point A^* is set consistent with critical operation of the inlet.

To compare an IRDCR with a scramjet and a ramjet, it is convenient and reasonable to use the same inlet operating characteristics, except that the total captured air flow, rather than a proportionate part, is compressed to either condition *ci* in a scramjet or $\bar{2}$ in the cowl lip plane of a ramjet. For the scramjet, normal (radially inward from the wall) fuel injection is assumed and the same assumptions as in the IRDCR regarding $\int p_w dA$, $\tau_w A_w$, and Q_w were made. For the ramjet combustor, operation consistent with that of the IRDCR gas generator, except over the range $0 \le ER \le 1$, as typified in Fig. 8, is used. With these assumptions, the combustor exit area ratios can be compared for the three cycles. Table 1 summarizes the results.

Note that for all inlet configurations at $M_0 = 4$ with an overall $ER = 1$, A^*/A_i for the ramjet is smaller than A_{ce}/A_i for the IRDCR which, in turn, is smaller than A_{ce}/A_i for the scramjet. Thus, for a given engine exit-to-inlet area ratio A_{ex}/A_i, the nozzle area ratio is greatest for the ramjet (A_{ex}/A^*) and smallest for the scramjet (A_{ex}/A_{ce}). Since $M^* = M_{ce} = 1$ at $M_0 = 4$ with an overall $ER = 1$, the ramjet will produce the greatest thrust and the scramjet the least. For all other conditions $M_{ce} > 1$ in both IRDCR and the scramjet, and the relative thrusts are not known a priori.

Engine Performance

Engine performance calculations were made at $M_0 = 4$, 5, 6, and 7 for each inlet configuration and engine cycle for overall equivalence ratios of 0 to 1. The net thrust coefficient is defined as

$$C_F = C_T - C_{D,\text{add}} \tag{10}$$

where

$$C_T = (1/q_0 A_i)\left[(\rho u^2 A)_{ex} - (\rho u^2 A)_0 + A_{ex}(p_{ex} - p_0)\right] \tag{11}$$

$$C_{D,\text{add}} = \frac{1}{q_0 A_i}\int_{A_0}^{A_i} (p - p_0)\, dA \tag{12}$$

Note that the engine inlet area A_i is used to normalize the thrust and drag coefficients and that the engine exit area A_{ex} is assumed to be 25% larger than A_i, i.e., $A_{ex}/A_i = 1.25$. Since the engine efficiency is determined by the fuel flow rate for a given thrust, $\dot{w}_f$ rather than *ER* is the appropriate parameter to hold constant when comparing the net thrusts of various configurations. Accordingly, C_F has been plotted against the normalized fuel flow parameter $\dot{w}_f/q_0 A_i$ in Figs. 11-13, which show the results for the three engine cycles at $M_0 = 4$ and $M_0 = 7$. Grids of net specific impulse, defined as

$$I_{spn} = C_F q_0 A_i / \dot{w}_f \tag{13}$$

have been added to these figures to facilitate quantitative comparison of engine efficiencies. Since the air capture ratio at a given $M_0 < 7$ varies with the inlet configuration, the maximum fuel flow rate, which corresponds to operation at $ER = 1.0$, will also vary with the inlet configuration; this variation is evident in Figs. 11-13 for $M_0 = 4.0$.

Figure 11 shows that at $M_0 = 4$ the maximum thrust can be obtained with inlet A and that inlets B and C are most efficient, that is, for the same C_F they require the lowest $\dot{w}_f$. At $M_0 = 7$, with the exception of inlet configuration E at low C_F, both thrust and efficiency increase with inlet compression. Thus, an unambiguous selection of the "best" inlet con-

Table 1 Area ratios[a] for IRDCR, scramjet, and ramjet

Engine	Inlet configuration	A_{ci}/A_i	A^*/A_i	A_{ce}/A_{ci}	A_{ce}/A_i
IRDCR	Cone	0.2439	0.1405	2.555	0.6232
	A	0.1830	0.1080	2.630	0.4813
	B	0.1473	0.0879	2.690	0.3912
	C	0.1153	0.0746	2.765	0.3186
	D	0.0717	0.0458	2.985	0.2140
	E	0.0499	0.0329	3.155	0.1575
Scramjet	Cone	0.3221		2.065	0.6651
	A	0.2424		2.120	0.5138
	B	0.1954		2.175	0.4250
	C	0.1531		2.235	0.3422
	D	0.0953		2.445	0.2333
	E	0.0665		2.620	0.1742
Ramjet	Cone		0.5833		
	A		0.4446		
	B		0.3621		
	C		0.2878		
	D		0.1864		
	E		0.1334		

[a] Geometries set by conditions at $M_0 = 4$ with an overall $ER = 1$.

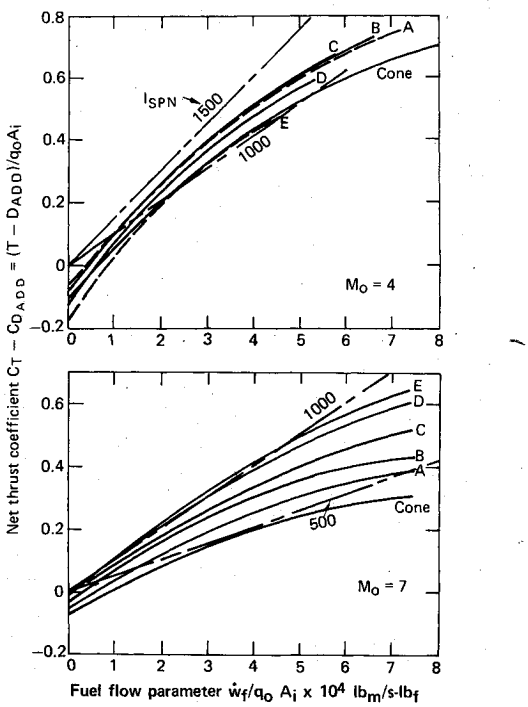

Fig. 11 Net thrust coefficients for IRDCR at $\alpha = 0$, $q_0 = 5000$ lb_f/ft^2.

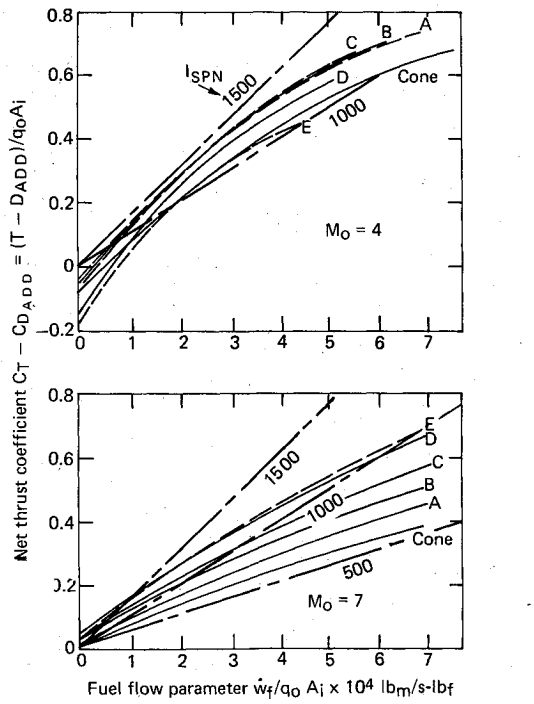

Fig. 12 Net thrust coefficients for supersonic combustion ramjet at $\alpha = 0$, $q_0 = 5000$ lb_f/ft^2.

iguration is not possible, although the choice appears to be in he C-D range and the cone and configuration A could cer-ainly be eliminated. The issue could only be resolved by examining climbout and cruise trajectories for a particular vehicle design and mission requirement. The low maximum hrust and efficiency of configuration E at $M_0 = 4$ could or ould not be acceptable, depending on these requirements.

The results for the scramjet shown in Fig. 12 are quite imilar to those for IRDCR. At $M_0 = 4$ efficiencies and thrust evels are slightly lower at high C_F and slightly higher at low C_F than for IRDCR. At $M_0 = 7$, efficiencies and thrust levels re greater for the scramjet for all inlet configurations. Positive values of C_F at $\dot{w}_f = 0$ arise from the fact that the nternal losses in a scramjet with the engine out are very low nd if A_{ex} is significantly larger than A_i then the exit stream thrust can be larger than the inlet stream thrust. In this case $A_{ex}/A_i = 1.25$ and $C_{D,add} = 0$ at $M_0 = 7$ which, with the other assumptions, leads to $C_F > 0$ at $\dot{w}_f = 0$.

Figure 13 shows the ramjet characteristics to be significantly different. At $M_0 = 4$, maximum thrust corresponds to a minimum contraction ratio inlet, but the efficiency is approximately invariant for all inlets. At $M_0 = 7$, increasing inlet contraction leads both to higher maximum thrust and increased efficiency.

To examine the relative merits of IRDCR with a ramjet and a scramjet over the selected Mach number range of 4-7, the vehicle thrust requirements must be defined for particular climbout and cruise trajectories. In general, for a relatively low thrust requirement in climb and acceleration and a long cruise at constant speed the IRDCR and the scramjet will

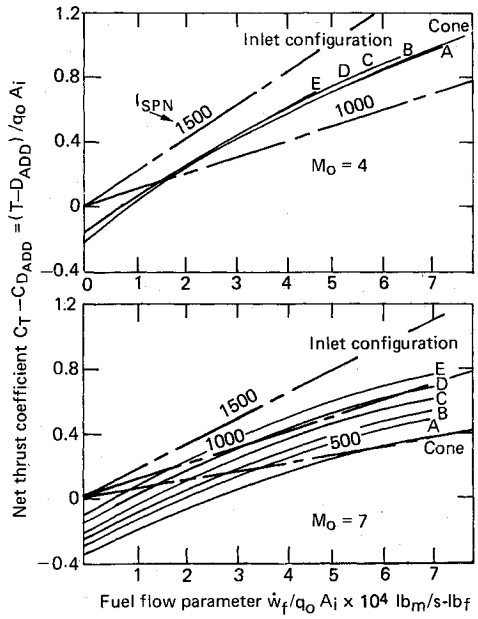

Fig. 13 Net thrust coefficients for subsonic combustion ramjet at $\alpha = 0$, $q_0 = 5000$ lb_f/ft^2.

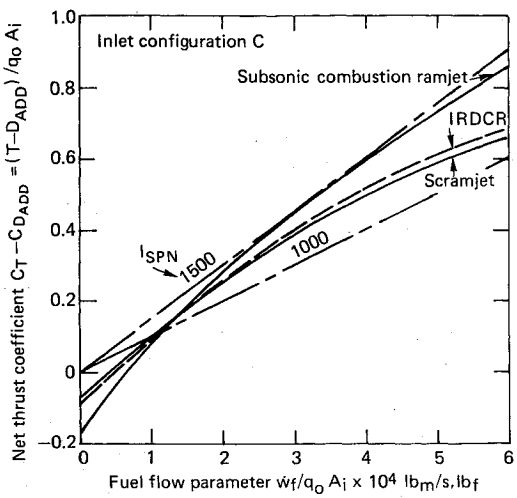

Fig. 14 Performance comparison at $M_0 = 4$ at $\alpha = 0$, $q_0 = 5000$ lb_f/ft^2.

require less fuel than the ramjet for a given range. Figures 14 and 15, which compare the thrust coefficient vs fuel parameter for inlet configuration C at M_0 of 4 and 7 for the three cycles, help to clarify this issue. At $M_0 = 4$, the curves for IRDCR and scramjet cross the ramjet curve at $\dot{w}_f/q_0 A_i = 1.3 \times 10^{-4}$ $lb_m/s\text{-}lb_f$, which corresponds to $ER = 0.25$, $C_F = 0.14$. At $M_0 = 7$ the crossover point with the IRDCR is at $\dot{w}_f/q_0 A_i = 4.37 \times 10^{-4}$ $lb_m/s\text{-}lb_f$ or $ER = 0.59$ and $C_F = 0.37$, and with the scramjet at $\dot{w}_f/q_0 A_i = 4.92 \times 10^{-4}$ $lb/s\text{-}lb_f$ or $ER = 0.67$ and $C_F = 0.43$. This trend of an increasing ER with increasing M_0 at the crossover point has been noted previously (see e.g., Refs. 16 and 17) but occurs at different ER values for other fuels and/or engine configurations. Generally, for $M_0 > 7.5$-8 cycles with supersonic combustion have higher efficiency than subsonic combustion ramjets at all ER values. It should be noted that the selected mass fraction of 0.25 to the gas generator and the setting of the geometries by conditions at $M_0 = 4$ with overall $ER = 1$ lead to the better performance of IRDCR at lower M_0 and poorer performance at high M_0 relative to the scramjet. Had these parameters been modified, the trend with M_0 could have been adjusted to suit the application.

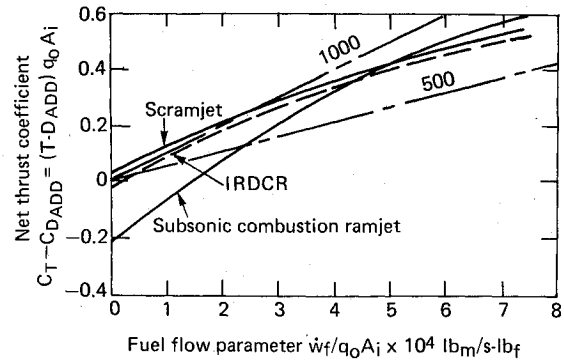

Fig. 15 Performance comparison at $M_0 = 7$ at $\alpha = 0$, $q_0 = 5000$ lb_f/ft^2, inlet configuration C.

Most applications, however, that require the high efficiency of airbreathing engines at $M_0 > 5$ include long cruise ranges corresponding to low C_F, hence the IRDCR or the scramjet turn out to give higher overall performance. For example, at $M_0 = 7$ a typical C_F at cruise is 0.2. From Fig. 15 the values of $\dot{w}_f/q_0 A_i$ are 1.7×10^{-4}, 2.1×10^{-4}, and 2.9×10^{-4} $lb/s\text{-}lb_f$ for the scramjet, the IRDCR and the ramjet, respectively, thus IRDCR would get 38% and scramjet would get 71% more cruise range than the ramjet for the same amount of fuel.

Concluding Remarks

The results of this analysis clearly depict the intimate relationship that exists between the inlet, gas generator, and supersonic combustor in the IRDCR. The methodology presented provides a means for quantitatively determining the exit areas of the gas generator and scramjet and assessing the effects on performance of each of the engine components. Caution should be exercised in generalizing the results, in that the family of inlets chosen for the study and the criteria used to select the range of operating conditions, although typical, are arbitrary. In particular, the air capture, pressure recovery, and design Mach number characteristics of other inlets and their effect on performance need to be examined in detail. Moreover, the feasibility of a particular inlet design involves many other considerations, including viscous effects, operation at angle of attack, cowl drag, etc. None of these was considered herein.

The principle advantages of this propulsion concept are the potential solution of a fundamental combustion limitation of the scramjet and the flexibility in engine cycle design which may prove to be an important asset in adapting an airbreather to a broad speed range variable mission profile requirement.

Acknowledgments

This work was supported by the U.S. Navy under Naval Sea Systems Command Contract N000-24-78-C-5384. The authors are greatly indebted to James L. Keirsey of The Johns Hopkins University, Applied Physics Laboratory, who is responsible for developing the basic concept of the IRDCR cycle.

References

[1] Billig, F.S. and Dugger, G.L., "The Interaction of Shock Waves and Heat Addition in the Design of Supersonic Combustors," *Twelfth Symposium (International) on Combustion,* The Combustion Institute, Pittsburgh, Pa., 1969, pp. 1125-1134.

[2] Billig, F.S., Dugger, G.L., and Waltrup, P.J., "Inlet-Combustor Interface Problems in Scramjet Engines," invited paper presented at the 1st International Symposium on Air Breathing Engines, Marseille, France, June 1972.

[3] Waltrup, P.J. and Billig, F.S., "The Structure of Shock Waves in Cylindrical Ducts," *AIAA Journal,* Vol. 11, Oct. 1973, pp. 1404-1408.

[4]Waltrup, P.J. and Billig, F.S., "Prediction of Precombustion Wall Pressure Distributions in Scramjet Engines," *Journal of Spacecraft and Rockets,* Vol. 10, Sept. 1973, pp. 620-622.

[5]Billig, F.S., Orth, R.C., and Funk, J.A., "Direct Connect Tests of a Hydrogen-Fueled Supersonic Combustor," NASA CR-1904, Aug. 1971.

[6]Waltrup, P.J., Anderson, G.Y., and Stull, F.D., "Supersonic Combustion Ramjet (SCRAMJET) Engine Development in the United States," Preprint 76-042, *The 3rd International Symposium on Air Breathing Engines,* The Johns Hopkins University Applied Physics Laboratory, March 1976.

[7]Heins, A.E., Jr., Reed, G.J., and Woodgrift, K.E., "Hydrocarbon Scramjet Feasibility Program Part III. Free Jet Engine Design and Performance," AFAPL TR-70-4, Jan. 1971.

[8]Kay, I.W., McVey, J.B., Kepler, C.E., and Chiappetta, L., "Hydrocarbon Fueled Scramjet Vol. VIII, Piloting and Flame Propagation Investigation," AFAPL TR 68-146, May 1971.

[9]Mestre, A. and Ducourneau, F., "Recent Studies on the Spontaneous Ignition of Rich Air-Kerosine Mixtures," Office National d'Etudes et de Recherches Aérospatiales (ONERA) TP 1209, Chatillon, France, 1973.

[10]Fehlner, L.F. and Nice, E.V., "Tabulation of Standard Atmospheres at 100 Foot Intervals of Altitude," The Johns Hopkins University Applied Physics Laboratory, TG 313-1, Aug. 1958.

[11]Billig, F.S., Waltrup, P.J., and Dale, L.A., "Combustor Performance Parameters for Hydrocarbon Fuels," The Johns Hopkins University Applied Physics Laboratory, TG-1246, May 1974.

[12]Cruise, D.R., "Notes on the Rapid Computation of Chemical Equilibria," *Journal of Physical Chemistry,* Vol. 68, No. 12, 1964, pp. 3797-3802.

[13]Billig, F.S. and Grenleski, S.E., "Experiments and Analysis of Heat Transfer in Supersonic Combustion Processes," *Fourth International Heat Transfer Conference, Paris, Versailles, August 1970,* Vol. 3, Elsevier Publishing Company, Amsterdam, 1970, pp. FC 6.1 1-11.

[14]Mager, A., "On the Model of Free, Shock Separated Turbulent Boundary Layer," *Journal of the Aeronautical Sciences,* Vol. 23, Feb. 1956, pp. 181-184.

[15]Crocco, L., "One-Dimensional Treatment of Steady Gas Dynamics," *Fundamentals of Gas Dynamics, Vol. III of High Speed Aerodynamics and Jet Propulsion,* Princeton University Press, 1958, p. 105.

[16]Dugger, G.L. and Billig, F.S., "Ramjet Technology, Chapter 11 Hypersonic Ramjets," The Johns Hopkins University Applied Physics Laboratory, TG-610-11, March 1970.

[17]Billig, F.S., "Design of Supersonic Combustors Based on Pressure-Area Fields," *Eleventh Symposium (International) on Combustion,* The Combustion Institute, Pittsburgh, Pa., 1978, pp. 755-769.